

Chapter 2

Phosphors for White-Light LEDs Through the Principle of Energy Transfer

Teng-Ming Chen and Yoan-Jen Yang

Abstract This chapter is an attempt to investigate and develop single-phased white light-emitting phosphors essentially for potential applications in white light-emitting diodes (WLEDs) based on the principle of resonant-type energy transfer. We first review the fundamentals of energy-transfer processes and propose a set of semi-empirical protocols for the design of white-emitting phosphors on the basis of bonding nature of hosts and the resonant-type energy transfer. The luminescent properties and energy-transfer processes for four categories of single-phased white light-emitting phosphors and a multi-composition phosphor are used as examples and discussed in detail. In summary, white-light emission can be realized by adopting single-composition two-complementary systems such as blue/yellow-emitting ($\text{CaAl}_2\text{Si}_2\text{O}_8\text{:Eu}^{2+}, \text{Mn}^{2+}$), cyan/red-emitting ($\text{BaGa}_4\text{S}_7\text{:Eu}^{2+}, \text{Mn}^{2+}$), or green-yellow/red-emitting phosphor ($\text{Ba}_2\text{ZnS}_3\text{:Ce}^{3+}, \text{Eu}^{2+}$) under blue or ultraviolet (UV) excitation. On the other hand, white-light emission can also be realized in three-primary phosphors such as blue/green/red-emitting $\text{SrZn}_2(\text{PO}_4)_2\text{:Eu}^{2+}, \text{Mn}^{2+}$ under blue excitation. Furthermore, the most intriguing examples of white-light generation with a high color-rendering index through resonant energy transfer are trichromatic inorganic phosphors such as $\text{Ca}_3\text{Y}(\text{GaO})_3(\text{BO}_3)_4\text{:Ce}^{3+}, \text{Mn}^{2+}, \text{Tb}^{3+}$, $\text{Mg}_2\text{Y}_8(\text{SiO}_4)_6\text{O}_2\text{:Ce}^{3+}, \text{Mn}^{2+}, \text{Tb}^{3+}$, $\text{NaCaBO}_3\text{:Ce}^{3+}, \text{Mn}^{2+}, \text{Tb}^{3+}$, and $\text{BaMg}_2\text{Al}_6\text{Si}_9\text{O}_{30}\text{:Eu}^{2+}, \text{Tb}^{3+}, \text{Mn}^{2+}$, which can effectively convert UV, near-UV, or blue light into a combination of RGB. To support and confirm the occurrence of energy transfer from a sensitizer (energy donor) to an activator (energy acceptor), one must provide two evidences, namely, spectral overlapping between a sensitizer and activator from steady-state spectra and shortening of luminescence decay rate of a sensitizer with increasing content of an activator. With transient spectra of the white-emitting phosphors, the mechanism of electrical multipolar resonance-type energy transfer can also be deduced.

T.-M. Chen (✉) · Y.-J. Yang

Phosphors Research Laboratory, Department of Applied Chemistry,
National Chiao Tung University, Hsinchu 30010, Taiwan
e-mail: tmchen@mail.nctu.edu.tw

© Springer-Verlag Berlin Heidelberg 2017

R.S. Liu (ed.), *Phosphors, Up Conversion Nano Particles, Quantum Dots and Their Applications*, DOI 10.1007/978-3-662-52771-9_2

2.1 Introduction

White light-emitting diodes (LEDs) have been recognized as green lightings for the next generation to replace conventional lamps and backlights due to the advantages of their low power consumption and being free of mercury. Although white light could be generated by two or three complementary LED chips at least, the cost of production is higher. Therefore, the economical method to produce white light is one-wavelength LED-converted phosphor, such as blue LED-pumped yellow $\text{Y}_3\text{Al}_5\text{O}_{12}:\text{Ce}^{3+}$ (YAG:Ce) [1]. However, the color-rendering index (R_a) of a white-light source made by the complementary blue and yellow emission is deficient because of the lack of red-light contribution resulting in nonrealization of the true color rendition. Hence, several red phosphors were developed to add into the above-mentioned system to improve the R_a value [2–5]. Unfortunately, the extreme difference in degradation between different host phosphors will produce color aberration. Accordingly, it is important to investigate a single-host phosphor with green-to-red emission bands for blue LEDs. The best choices of activators in phosphors are the ions with $f-d$ or $d-d$ electron configurations because they could emit visible and broad-band light under the influence of crystal field and nephelauxetic effect [6, 7]. Furthermore, a phosphor could emit a couple of radiation by co-doping these ions in a single host such as $\text{Eu}^{2+}/\text{Mn}^{2+}$ [8–18], $\text{Ce}^{3+}/\text{Eu}^{2+}$ [19–21], and $\text{Ce}^{3+}/\text{Mn}^{2+}$ [22], and the energy transfer would exist between activators in a phosphor by effective resonant-type by way of a multipolar interaction [8, 9]. Nevertheless, in the past few years, coactivated single-composition phosphors with blue absorption or for blue LEDs have rarely been investigated. In this chapter, we will review a single-phased phosphor, $\text{Ce}^{3+}/\text{Eu}^{2+}$ co-doped Ba_2ZnS_3 , which shows ultraviolet-to-blue absorption and green-to-red emission, thus exhibiting great potential for application in white LEDs while a blue chip is coupled.

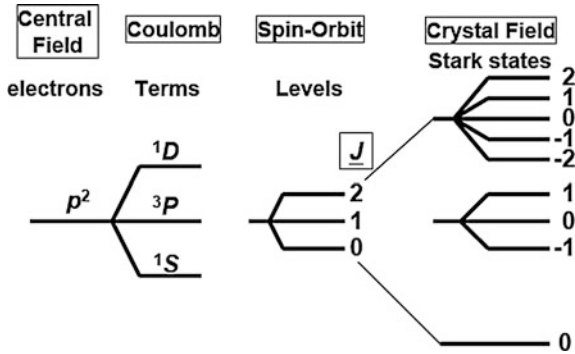
2.2 Theory of Electronic Transition and Luminescence

An inorganic phosphor is composed of a host lattice and an activator, and sometimes a sensitizer is also required. The host usually comprises a combination of optically inert cations and anions; the activator generally comprises optically active cations.

The energy levels of an activator can be defined by the spectroscopic term, $^{2S+1}L_J$, where S is the spin-angular momentum; L is orbital angular momentum; and J is the spin-orbit angular momentum. The Hamiltonian (H) of an activator could be written as

$$H_{\text{activator}} = H_o + H_c + H_{so} + H_{cf} \quad (2.1)$$

Fig. 2.1 Hamiltonians for a carbon atom with $1s^2 2s^2 2p^2$ configuration [4]. Reprinted from Ref. [4]. Copyright 2004, with permission from Elsevier



where H_o is the central field Hamiltonian; H_c is the coulomb Hamiltonian; H_{so} is the spin-orbit Hamiltonian; and H_{cf} is crystal field Hamiltonian.

As shown in Fig. 2.1, the diagram gives the relation between various Hamiltonians. The allowed transitions are governed by the following selection rules:

$$L = \pm 1; \quad S = 0; \quad J = \pm 1, 0$$

but not $J = 0$ to $J = 0$. In fact, these selection rules are only suitable for dipole transitions, i.e., transitions between electric dipole states. In addition, other possible multipolar states can exist as magnetic dipoles, electric quadrupoles, magnetic quadrupoles, and higher multipole orders. The easiest way to visualize the types of multipoles is to imagine a p -electron as shown in Fig. 2.2.

The electric field vector \vec{F} , directs at the greatest electron field density. On the contrary, the magnetic field vector \vec{M} , is at right angles to that density. Therefore, the transition intensities between the electric and magnetic multipoles are lower than those involving electric-to-electric multipoles. Moreover, one pole can influence another at fair distances in a lattice, and this is called an “electric multipolar interaction” [4]. The transition probability can be written as [7]

Fig. 2.2 Diagrams for electropole radiators. Reprinted from Ref. [4]. Copyright 2004, with permission from Elsevier

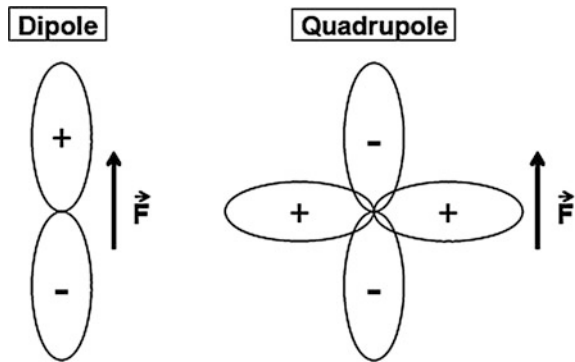
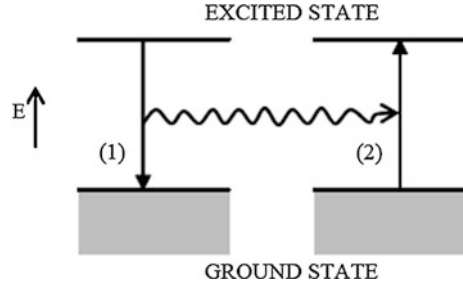


Fig. 2.3 Diagram of virtual photon exchange between activators. Reprinted from Ref. [4]. Copyright 2004, with permission from Elsevier



$$(P_k)_{fi} = \langle \Psi_f^* | M | \Psi_i \rangle$$

where M is the operator form of a multipole. Accordingly, the types of multipoles are related to the orientations of electric or magnetic field.

The energy-transfer mechanisms between activators could be classified into radiative and nonradiative types chiefly. Radiative energy transfer occurs between the two activators, A_1 and A_2 , separated by a few unit-cell distances. A_1 absorbs enough energy to be excited, and then it will emit a photon, which may be captured by an adjacent activator, A_2 , which then also becomes excited. Therefore, the radiative energy transfer could be labeled as virtual photon exchange as shown in Fig. 2.3. The nonradiative energy transfer is also classified into resonance-energy transfer (RET), spin-coupling energy exchange (SCEE), and non-resonance-energy transfer (NRET) [4].

Resonance energy transfer occurs between a sensitizer (S) and an activator (A) with the same radiative frequency, and the mechanism could be of exchange interaction or electric multipolar interaction.

In fact, the phenomenon of energy transfer could be demonstrated by the overlap of emission spectrum of S and excitation spectrum of A. Dexter's energy transfer formula is described as [8]:

$$P_{SA} = 2\pi/\hbar |\langle S, A^* | H_{SA} | S^*, A \rangle|^2 \int F_S(E) F_A(E) dE \quad (2.2)$$

where the integral describes the spectral overlap; $F_S(E)$ and $F_A(E)$ represent the normalized shapes of the sensitizer and activator, respectively; the matrix element represents the interaction between initial state $|S^*, A\rangle$ and final state $\langle S, A^*|$; H_{SA} is the Hamiltonian of the interaction; P_{SA} is the probability of energy transfer and, when the spectral overlap is absent, the phenomenon of resonance energy-transfer vanishes, as shown in Figs. 2.4 and 2.5, respectively. Furthermore, the energy-transfer probability is related to the type of interaction. For electric multipolar interaction, the distance dependence is given by $R^{-\alpha}$ where α is 6 and 8 corresponding to electric dipole-dipole and dipole-quadrupole interactions,

Fig. 2.4 Diagram of the energy transfer between a sensitizer and an activator. Reprinted from Ref. [5], with kind permission from Springer Science+Business Media

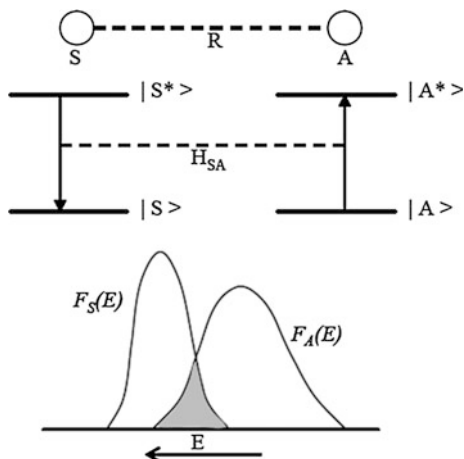
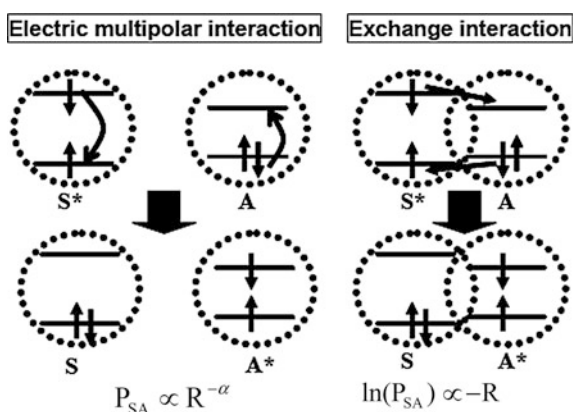


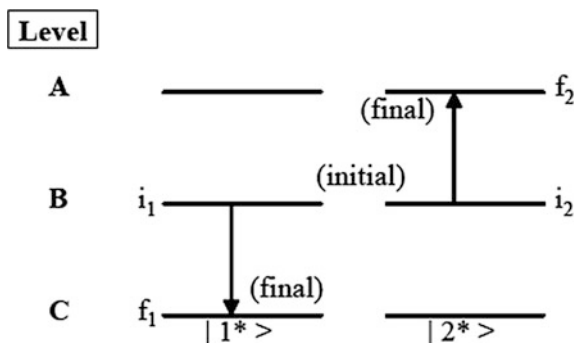
Fig. 2.5 Diagrams of the energy-transfer mechanisms of electric multipolar and exchange interactions



respectively. For exchange interaction, the distance dependence is exponential, and the wavefunction overlap between S and A is required [8, 9].

On the other hand, spin-coupling energy exchange occurs between two adjacent activators, A_1 and A_2 , which are no further than approximately two to three lattice sites apart [4]. As shown in Fig. 2.6, the initial state of A_1 and A_2 are both in the excited state, and they exchange energy by way of spin-coupling. Finally, A_1 returns to ground state, and A_2 transits to a higher level doubling that of initial state. The process is usually observed in the activators, which can absorb infrared radiation, which is then converted to visible light (also called an “anti-Stokes process”).

Fig. 2.6 Diagram of spin-coupling energy exchange. Reprinted from Ref. [4]. Copyright 2004, with permission from Elsevier



2.2.1 Literature Review

It is well-known that energy transfer mostly occurs between a sensitizer and an activator in a phosphor, e.g., $\text{Eu}^{2+}/\text{Mn}^{2+}$, $\text{Ce}^{3+}/\text{Eu}^{2+}$, $\text{Ce}^{3+}/\text{Mn}^{2+}$, $\text{Ce}^{3+}/\text{Tb}^{3+}/\text{Mn}^{2+}$, $\text{Eu}^{2+}/\text{Tb}^{3+}/\text{Mn}^{2+}$, and so on. The activator acts as an efficient sensitizer to transfer energy to the co-doped activator. In 1970, Barry observed that an effective energy transfer from Eu^{2+} to Mn^{2+} occurred in $\text{BaMg}_2\text{Si}_2\text{O}_7:\text{Eu}^{2+}$, Mn^{2+} phosphor, in which Eu^{2+} and Mn^{2+} occupied the Ba^{2+} and Mg^{2+} sites, respectively [10]. In the 1980s, Rubio et al. reported that energy transfer from Eu^{2+} to Mn^{2+} took place in the sodium halide lattices, in which Eu^{2+} and Mn^{2+} formed close pairs [11–14]. In the 1990s, Caldino et al. described that the $\text{Eu}^{2+} \rightarrow \text{Mn}^{2+}$ energy transfer process occurred by way of an electric dipole–quadrupole or exchange interaction in the small Eu–Mn clusters formed in the calcium halide and KBr crystals [15–17]. In 1996, Lin et al. discussed the energy-transfer process between the luminescent centers in $\text{Ca}_8\text{Zn}(\text{SiO}_4)_4\text{Cl}_2:\text{Eu}^{2+}$, Mn^{2+} phosphor and demonstrated the substitution of Eu^{2+} and Mn^{2+} for Ca^{2+} and Zn^{2+} sites, respectively [18]. In 1999, Tan et al. determined that the $\text{Ce}^{3+} \rightarrow \text{Eu}^{2+}$ energy transfer in BaLiF_3 occurs by way of a dipole–dipole interaction [19]. In 2002, Najafov et al. observed that the energy-transfer process from Ce^{3+} to Eu^{2+} in CaGa_2S_4 is a dipole–dipole interaction [20]; Lin et al. found that the energy-transfer mechanism from Ce^{3+} to Eu^{2+} in $\text{Ca}_8\text{Mg}(\text{SiO}_4)_4\text{Cl}_2$ is electric dipole–dipole interaction [21]. In 2003, Caldino discussed that the energy-transfer mechanisms between $\text{Ce}^{3+}/\text{Eu}^{2+}$ and $\text{Ce}^{3+}/\text{Mn}^{2+}$ in CaF_2 are of the electric dipole–dipole type and electric dipole–quadrupole type, respectively [22]. Until recently, single-composition phosphors under UV and blue radiations have rarely been investigated for the fabrication of white LEDs. In 2004, Setlur et al. declared that $\text{Sr}_2\text{P}_2\text{O}_7:\text{Eu}^{2+}$, Mn^{2+} and $\text{Ca}_5(\text{PO}_4)_3\text{F}:\text{Eu}^{2+}$, Mn^{2+} phosphors could be excited by UV/blue LEDs and produce white-light emission [23]. Kim et al. reported that $\text{Ba}_3\text{MgSi}_2\text{O}_8:\text{Eu}^{2+}$, Mn^{2+} [24] and $\text{Sr}_3\text{MgSi}_2\text{O}_8:\text{Eu}^{2+}$, Mn^{2+} [25] phosphors could be pumped by 375-nm InGaN LED chips to generate white light. In 2011, Huang and Chen reported a novel single-phased trichromatic white-emitting $\text{Ca}_3\text{Y}(\text{GaO})_3(\text{BO}_3)_4:\text{Ce}^{3+}$, Mn^{2+} , Tb^{3+} for UV-LEDs and studied the energy transfer from $\text{Ce}^{3+} \rightarrow \text{Mn}^{2+}$ as well as the green emission from Tb^{3+} [26].

Zhang and Gong reported a series of single-phased white-emitting $\text{NaCaBO}_3\text{:Ce}^{3+}$, Tb^{3+} , Mn^{2+} phosphors and proposed them for LED applications [27]. Lü et al. reported a tunable full-color trichromatic-emitting $\text{BaMg}_2\text{Al}_6\text{Si}_9\text{O}_{30}\text{:Eu}^{2+}$, Tb^{3+} , Mn^{2+} phosphor, in which white light can be generated from RGB emissions with blue at 450 nm, green at 542 nm, and red at 610 nm, respectively, through $\text{Eu}^{2+} \rightarrow \text{Tb}^{3+}$ and $\text{Eu}^{2+} \rightarrow \text{Mn}^{2+}$ energy-transfer processes [28].

Consequently, this has triggered many active research efforts devoted to the quest for new UV/blue LED-converting single-phased and white-emitting phosphors. In the following sections we will describe and discuss the principle of white-light generation for four categories of single-phased white-emitting phosphors.

2.3 Design Principles and Preparation Protocol of White-Emitting Phosphors

Regarding the design of single-phased white-emitting phosphors for UV/blue LEDs, we will describe two groups of commonly encountered materials as examples, namely, oxides and sulfides. The activators generally selected are Eu^{2+} , Ce^{3+} and Mn^{2+} ions because their emission wavelengths are tunable by changing coordination environment and site symmetry as well as the emission spectra exhibit broadband. According to the effective ionic radii of cations with different coordination number reported by Shannon [29], we propose that Eu^{2+} and Ce^{3+} ions tend to occupy the Ca^{2+} , Sr^{2+} and Ba^{2+} sites, and Mn^{2+} ions reasonably substitute for the Ca^{2+} , Sr^{2+} , Ba^{2+} , Mg^{2+} , and Zn^{2+} site and emit green and red light when occupying the four- and six-coordinated lattice sites in a dual-element oxide matrix, respectively [5]. However, in an oxide matrix with more than two elements, the Mn^{2+} ions are affected by not only substitution sites but also adjacent cations, generally resulting in emission in the green-to-red spectral range. Therefore, based on semiempirical results, we propose flowcharts for the design and preparation of white-emitting oxide and sulfide phosphors for blue LEDs; these flowcharts are summarized in Fig. 2.7, respectively.

For sulfide phosphors, the host lattices are mostly tri-element compounds in nature, and they can be represented by $\text{M}'_a\text{M}''_b\text{S}_m$, where M' and M'' can be selected from the following:

$$\begin{aligned}\text{M}' &: \text{Ca}^{2+}, \text{Sr}^{2+} \text{ and } \text{Ba}^{2+} \\ \text{M}'' &: \text{Al}^{3+}, \text{Ga}^{3+}, \text{In}^{3+}, \text{Mg}^{2+} \text{ and } \text{Zn}^{2+}\end{aligned}$$

In the sulfide matrix, due to the influence of the nephelauxetic effect resulting from the lower electronegativity of sulfur atom, the energy level of center of gravity of the d level of an activator is lower than that in oxide matrix. Accordingly, Eu^{2+}

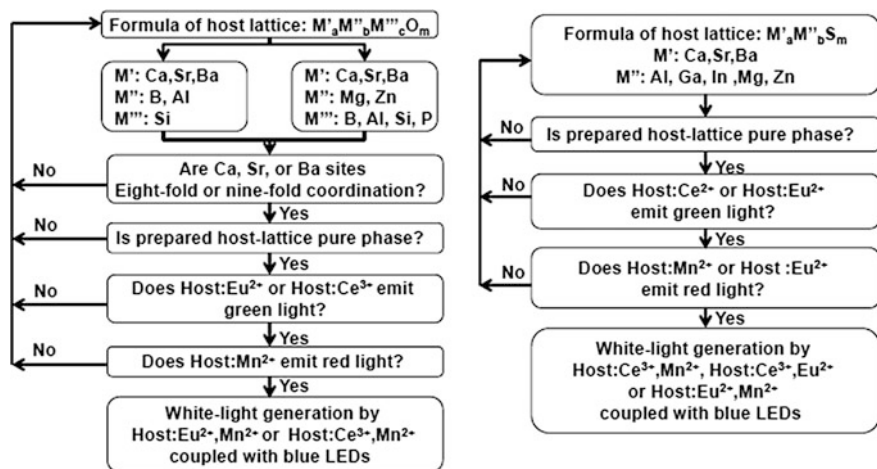


Fig. 2.7 Flow diagram describing the design of white-emitting oxide and sulfide phosphors for blue LEDs

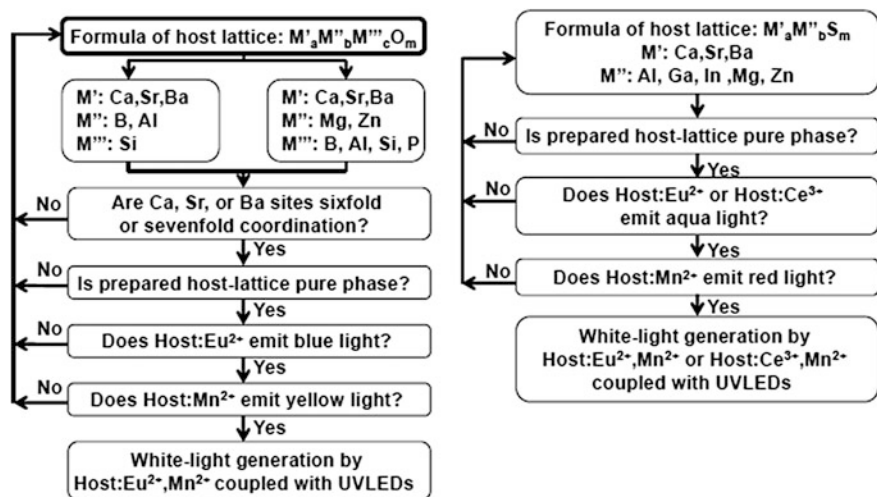


Fig. 2.8 Flow diagram describing the design of white-emitting oxide and sulfide phosphors for UVLED

could emit aqua to red light; Ce^{3+} ions could emit blue to green light; and Mn^{2+} ions could emit mostly red light.

Furthermore, the flowcharts of design and preparation of white-emitting oxide and sulfide phosphors for UV LEDs are also shown, respectively in Fig. 2.8.

According to the flowcharts showing the design and preparation protocol, we have demonstrated that the white-emitting phosphors for UV and blue LEDs can be obtained and used to generate white light. In addition, a series of trichromatic

white-emitting phosphor for UVLEDs has also been developed and will be discussed in the next section. The luminescence properties and energy-transfer mechanisms between two or among three luminescent centers have been widely investigated and is described in following sections.

2.4 White-Emitting Phosphors with Predesigned Energy-Transfer Mechanisms

To illustrate the principle of white light emission through the energy-transfer principle and to verify the proposed protocol of designing white-emitting phosphors, we will describe how white light is generated and give representative examples to demonstrate that white-emitting phosphors can be predesigned and realized using the energy-transfer principle.

2.4.1 *White-Emitting Phosphors with Energy Transfer from Eu^{2+} to Mn^{2+}*

It has been investigated that Eu^{2+} may serve as an efficient sensitizer that absorbs and transfers energy to Mn^{2+} in different host lattices. As reported in the literature, Caldino et al. reported the $\text{Eu}^{2+} \rightarrow \text{Mn}^{2+}$ energy-transfer process in the single crystals of $\text{CaCl}_2:\text{Eu}^{2+}, \text{Mn}^{2+}$ under photoexcitation. The investigators suggested that the Eu^{2+} -to- Mn^{2+} energy-transfer process observed in $\text{CaCl}_2:\text{Eu}, \text{Mn}$ can be rationalized by the formation of small complexes of Eu-Mn in the lattice [15, 16]. Similar energy transfer was also observed by Barry in the $\text{BaMg}_2\text{Si}_2\text{O}_7:\text{Eu}^{2+}, \text{Mn}^{2+}$ phosphor [10]. Yao et al. investigated the luminescence and decay lifetimes of $\text{BaMg}_2\text{Si}_2\text{O}_7:\text{Eu}^{2+}, \text{Mn}^{2+}$ as a function of Mn^{2+} concentrations and confirmed the occurrence of energy transfer from Eu^{2+} to Mn^{2+} [30]. Rubio et al. used an ionic radius criterion to predict pairing between two impurity dopant ions in alkali halide host matrix, which may provide a reasonable basis for selecting appropriate impurity dopant ions for developing efficient phosphor materials [12]. Furthermore, the $\text{Eu}^{2+} \rightarrow \text{Mn}^{2+}$ energy-transfer mechanism in $\text{KBr}:\text{Eu}^{2+}, \text{Mn}^{2+}$ phosphor was described by Mendez et al. [17] who proposed the possible formation of small $\text{Eu}^{2+}\text{-Mn}^{2+}$ clusters in the KBr lattice. Mendez et al. also proposed that the $\text{Eu}^{2+} \rightarrow \text{Mn}^{2+}$ energy transfer may be rationalized by assuming that a possible dipole-quadrupole or exchange (superexchange) interaction mechanism is active in the $\text{Eu}^{2+}\text{-Mn}^{2+}$ cluster formation [17]. Recently, Kim et al. reported that $\text{Ba}_3\text{MgSi}_2\text{O}_8:\text{Eu}, \text{Mn}$ can serve as a phosphor for fabrication of a warm-white LED [24]. They observed that with optimal excitation wavelength at 375 nm, $\text{Ba}_3\text{MgSi}_2\text{O}_8:\text{Eu}, \text{Mn}$ shows three emission bands centered at 442 nm from the first Eu^{2+} , 505 nm from the second Eu^{2+} , and 620 nm from Mn^{2+} [24], respectively. Table 2.1 summarizes a variety of representative examples of white-emitting

Table 2.1 Single-phased white-emitting phosphors with $\text{Eu}^{2+} \rightarrow \text{Mn}^{2+}$ energy transfer

Phosphor	$\text{CaAl}_2\text{Si}_2\text{O}_8\text{:Eu}^{2+}, \text{Mn}^{2+}$	$\text{SrZn}_2(\text{PO}_4)_2\text{:Eu}^{2+}, \text{Mn}^{2+}$	$\text{BaGa}_4\text{S}_7\text{:Eu}^{2+}, \text{Mn}^{2+}$	$\text{Ca}_2\text{MgSi}_2\text{O}_7\text{:Eu}^{2+}, \text{Mn}^{2+}$	$\text{BaMgSiO}_4\text{:Eu}^{2+}, \text{Mn}^{2+}$
Excitation range (nm)	280–395 (UV)	310–395 (UV)	330–390 (UV)	300–450 (B)	350–410 (UV-VIS)
Emission wavelength (nm)	425 (B), ~560 (Y)	416 (B), 538 (G), 613 (R)	475 (A), 653 (R)	~450 (B)-650 (R)	477 (B), 626 (O-R)
Energy transfer mechanism	Dipole–quadrupole	Dipole–quadrupole	Exchange	Dipole–quadrupole	Dipole–quadrupole and exchange
Energy transfer critical distance (Å)	10.8	11.4	5.9	11.90	9.46, 4.32
Reference	[31]	[32]	[33]	[34]	[35]
Phosphor	$\text{Ca}_{10}\text{K}(\text{PO}_4)_7\text{:Eu}^{2+}, \text{Mn}^{2+}$	$\text{Ca}_9\text{La}(\text{PO}_4)_7\text{:Eu}^{2+}, \text{Mn}^{2+}$	$\text{Ca}_9\text{Y}(\text{PO}_4)_7\text{:Eu}^{2+}, \text{Mn}^{2+}$	$\text{Ca}_9\text{Gd}(\text{PO}_4)_7\text{:Eu}^{2+}, \text{Mn}^{2+}$	$\text{Ca}_4\text{Si}_2\text{O}_7\text{F}_2\text{:Eu}^{2+}, \text{Mn}^{2+}$
Excitation range (nm)	250–420 (n-UV)	280–395 (UV)	310–395 (UV)	380 (n-UV)	240–500 (UV-Blue)
Emission wavelength (nm)	460 (B), 635 (O-R)	425 (B), ~560 (Y)	486 (B), 638 (R)	494 (B), 652 (O-R)	460 (B), 576 (Y-O)
Energy transfer mechanism	Dipole–quadrupole	Dipole–quadrupole	Dipole–quadrupole	Dipole–quadrupole	Dipole-quadrupole
Energy transfer critical distance (Å)	12.2	11.36	11.04	11.10	11.66
Reference	[36]	[37]	[38]	[39]	[40]

phosphors with energy transfer $\text{Eu}^{2+} \rightarrow \text{Mn}^{2+}$ reported in various hosts such as silicates, phosphates, oxyfluoride, and sulfide. In general, the white light consists of blue and yellow or blue/green/red radiations resulting from blue, near-UV, or ultraviolet light source pumping. Furthermore, the energy-transfer mechanism found in almost all the phosphors is of dipole–quadrupole type, which is supported by the critical distance of energy transfer indicated in Table 2.1, with a few cases being exchange type due to an intrinsic short interatomic distance between the sensitizer and the activator.

Table 2.2 Single-phased white-emitting phosphors with $\text{Ce}^{3+} \rightarrow \text{Eu}^{2+}$ energy transfer

Phosphor	Ba_2ZnS_3 : Ce^{3+} , Eu^{2+}	$\text{Sr}_3\text{Al}_2\text{O}_5\text{Cl}_2$: Ce^{3+} , Eu^{2+}	$\text{Ca}_2\text{BO}_3\text{Cl}$: Ce^{3+} , Eu^{2+}	$\text{Sr}_3\text{B}_2\text{O}_6$: Ce^{3+} , Eu^{2+}
Excitation range (nm)	400–450 (B)	320–370 (UV-nUV)	325–400 (UV-nUV)	365 (UV)
Emission wavelength (nm)	498–540 (GY), 655 (R)	438 (B), 583 (Y-O)	422 (B), 573 (Y)	434 (B), 574 (O-Y)
Energy transfer mechanism	Dipole–dipole	Dipole–dipole	Dipole–dipole	Dipole–dipole
Energy transfer critical distance (Å)	32.7	28.6	32.2	30
Reference	[36]	[37]	[38]	[39]

2.4.2 White-Emitting Phosphors with Energy Transfer from Ce^{3+} to Eu^{2+}

Table 2.2 summarizes several representative examples of single-phased white-emitting phosphors with energy transfer $\text{Ce}^{3+} \rightarrow \text{Eu}^{2+}$ reported in the literature. The host composition ranges in a variety from highly covalent sulfide, oxychloride, and more-ionic borate. The principle to generate white light generally employs phosphors that emit a couple of radiation by co-doping activators with f - d or d - d electron configurations such as $\text{Ce}^{3+}/\text{Eu}^{2+}$ [19–22] the energy transfer would essentially occur between activator/coactivator couples by effective resonant type by way of a multipolar interaction. As indicated in Table 2.2, we have observed that the white light consists of G/Y/R, B/Y/O, or B/Y radiations resulted from blue, near-UV, or ultraviolet light-source pumping, respectively. In addition, the energy-transfer mechanism determining the four phosphors is essentially of resonant dipole–dipole type with very long interatomic distances (i.e., ≥ 30 Å) between sensitizer Ce^{3+} and activator Eu^{2+} regardless of the type of host compound.

Yang and Chen [41] reported the $\text{Ba}_2\text{ZnS}_3:\text{Ce}^{3+}$, Eu^{2+} sulfide phosphor, which shows intense blue absorption and tunable green-to-red emission. The $\text{Ce}^{3+} \rightarrow \text{Eu}^{2+}$ energy transfer has been demonstrated to be resonant type by way of an electric dipole–dipole mechanism. Because $\text{Ba}_2\text{ZnS}_3:\text{Ce}^{3+}$, Eu^{2+} is able to generate white light under excitation at 420 nm, the CIE chromaticity coordinates were found to be (0.34, 0.49). The sulfide phosphor would be a great potential application as a blue radiation–converting phosphor for white LEDs. Chang also investigated a series of cold-and-warm white LEDs using the $\text{Sr}_3\text{Al}_2\text{O}_5\text{Cl}_2:\text{Ce}^{3+}, \text{Eu}^{2+}$ phosphor [42]. In the $\text{Ca}_2\text{BO}_3\text{Cl}:0.06\text{Ce}^{3+}, 0.01\text{Eu}^{2+}$ phosphor [43], the mechanism of resonance-type $\text{Ce}^{3+} \rightarrow \text{Eu}^{2+}$ energy transfer was established to be of an electric dipole–dipole nature, and the critical distance was estimated to be 31 Å based on the spectral overlap and concentration quenching model. A white light was obtained from $\text{Ca}_2\text{BO}_3\text{Cl}:0.06\text{Ce}^{3+}, 0.01\text{Eu}^{2+}$ phosphor with chromaticity coordinates (0.31, 0.29) and relative color temperature of 7,330 K on excitation with a wavelength of 360 nm, and therefore it is potentially a good candidate as an UV-convertible

phosphor for white LEDs. The $\text{Sr}_3\text{B}_2\text{O}_6\text{:Ce}^{3+}$, Eu^{2+} borate phosphors reported by Chang and Chen [44] exhibit varied hues from blue through white and eventually to yellow-orange via resonance-type $\text{Ce}^{3+} \rightarrow \text{Eu}^{2+}$ energy transfer by properly tuning the relative proportion of $\text{Ce}^{3+}/\text{Eu}^{2+}$. The investigators claimed that electric dipole–dipole interaction dominates the energy-transfer mechanism in $\text{Sr}_3\text{B}_2\text{O}_6\text{:Ce}^{3+}$, Eu^{2+} phosphor, and the critical distance of energy transfer has been estimated to be approximately 30 Å by both spectral-overlap and concentration-quenching methods. Under the excitation of UV radiation, white light is generated by coupling 434- and 574-nm emission bands attributed to Ce^{3+} and Eu^{2+} radiations, respectively.

2.4.3 White-Emitting Phosphors with Energy Transfer from Ce^{3+} to Mn^{2+} [45–48]

Table 2.3 summarizes four of the representative single-phased white-emitting phosphors with energy transfer from Ce^{3+} to Mn^{2+} . Hsu et al. described that in the PL/PLE spectra of $\text{MgY}_4\text{Si}_3\text{O}_{13}\text{:Ce}^{3+}$, Mn^{2+} , the increment of Mn^{2+} concentration would lead to a systematic decrease of Ce^{3+} emission due to the efficient $\text{Ce}^{3+} \rightarrow \text{Mn}^{2+}$ energy transfer [45], which occurs because of the spectral overlap between the emission band of Ce^{3+} and the excitation band of Mn^{2+} . The resonant $\text{Ce}^{3+} \rightarrow \text{Mn}^{2+}$ energy transfer is of the dipole–quadrupole type, which was supported by decay-lifetime data, and the critical distance of the energy transfer was calculated to be 14.13 Å. The color-tunable emission in $\text{Ce}^{3+}/\text{Mn}^{2+}$ co-doped system can be realized by continuous shifting of the emission colors from blue to white and eventually to the orange-red region. Müller and Jüstel investigated the photoluminescence and measured the transient spectral from 100 to 500 K to understand the thermal behavior of $\text{Ca}_3\text{Y}_2(\text{Si}_3\text{O}_9)_2\text{:Ce}^{3+}$, Mn^{2+} [46]. It turned out that the mechanism of $\text{Ce}^{3+} \rightarrow \text{Mn}^{2+}$ energy transfer is due to dipole–quadrupole interaction and $\text{Ca}_3\text{Y}_2(\text{Si}_3\text{O}_9)_2\text{:Ce}^{3+}$, Mn^{2+} also shows white emission and exhibits excellent thermal stability. Liu et al. reported a new tunable full color-emitting $\text{Ca}_3\text{Sc}_2\text{Si}_3\text{O}_{12}\text{:Ce}^{3+}$,

Table 2.3 Single-phased white-emitting phosphors with $\text{Ce}^{3+} \rightarrow \text{Mn}^{2+}$ energy transfer

Phosphor	$\text{MgY}_4\text{Si}_3\text{O}_{13}\text{:Ce}^{3+}$, Mn^{2+}	$\text{Ca}_3\text{Y}_2(\text{Si}_3\text{O}_9)_2\text{:Ce}^{3+}$, Mn^{2+}	$\text{Ca}_3\text{Sc}_2\text{Si}_3\text{O}_{12}\text{:Ce}^{3+}$, Mn^{2+}	$\text{Ca}_2\text{Gd}_8(\text{SiO}_4)_6\text{O}_2\text{:Ce}^{3+}$, Mn^{2+}
Excitation range (nm)	328 (UV)	300 (UV)	450 (B)	352 (UV)
Emission Wavelength (nm)	455 (B), 587 (O-R)	395 (V-B), 545 (Y-O)	574 (Y), 680 (R)	428 (B), 588 (R-O)
Energy transfer mechanism	Dipole–quadrupole	Dipole–quadrupole	Dipole–quadrupole	Dipole–quadrupole
Energy transfer critical distance (Å)	14.13	8.1, 8.8	NA	9.4
Reference	[45]	[46]	[47]	[48]

Mn^{2+} phosphor [47] by controlling the distribution of Mn^{2+} in the Ca^{2+} and Sc^{3+} lattice sites, respectively, through the addition of doped La^{3+} , Gd^{3+} , Lu^{3+} , and Y^{3+} lanthanides ions as charge compensators with the aid of $\text{Ce}^{3+} \rightarrow \text{Mn}^{2+}$ energy transfer. By using this single-phased $\text{Ca}_3\text{Sc}_2\text{Si}_3\text{O}_{12}:\text{Ce}^{3+}$, Mn^{2+} phosphor and blue (450 nm) InGaN LED chips, pcWLEDs with a high R_a of 91–92 and a color temperature of 5379–6954 K could be achieved [47]. Li et al. investigated the $\text{Ce}^{3+} \rightarrow \text{Mn}^{2+}$ energy transfer in $\text{Ca}_2\text{Gd}_8(\text{SiO}_4)_6\text{O}_2:\text{Ce}^{3+}$, Mn^{2+} phosphors [48] and demonstrated that the $\text{Ce}^{3+} \rightarrow \text{Mn}^{2+}$ transfer is of a resonant type by way of a dipole–quadrupole mechanism, and the critical distance calculated by the quenching-concentration and spectral-overlap methods are 9.4 and 9.2 Å, respectively. A color-tunable emission in $\text{Ca}_2\text{Gd}_8(\text{SiO}_4)_6\text{O}_2:\text{Ce}^{3+}$, Mn^{2+} phosphors can be realized by the modulation of excitation wavelengths, namely, the change of Ce^{3+} emission at different lattice sites and the relative PL intensity of Ce^{3+} and Mn^{2+} . Wide-ranging white light with varied hues was obtained in $\text{Ca}_2\text{Gd}_8(\text{SiO}_4)_6\text{O}_2:\text{Ce}^{3+}$, Mn^{2+} by utilizing the principle of energy transfer, properly designed activator contents, and the selection of excitation wavelength in the range of 287–352 nm [48].

2.4.4 *Trichromatic White-Emitting Phosphors with Dual-Energy Transfer*

Tremendous efforts have been made to generate white-light emission with a high color-rendering index (R_a) using inorganic phosphors to convert ultraviolet (UV), near-UV, or blue light into a combination of RGB. However, in the three-component (RGB) converting system, the manufacturing cost is high and the blue-emission efficiency poor because of the strong reabsorption of blue light by the red- and green-emitting phosphors. In an attempt to circumvent these disadvantages, there have been many investigations on efficient, durable, and single-phased white-emitting phosphors with RGB components (i.e., green from $\text{Ce}^{3+} \rightarrow \text{Tb}^{3+}$ and $\text{Eu}^{2+} \rightarrow \text{Tb}^{3+}$, red from $\text{Ce}^{3+} \rightarrow \text{Mn}^{2+}$ or $\text{Eu}^{2+} \rightarrow \text{Mn}^{2+}$) through energy-transfer couples, and this is drawing investigators' attention. Caldino et al. [22] first reported the $\text{Ce}^{3+} \rightarrow \text{Mn}^{2+}$ energy transfer and mechanism involved with $\text{CaF}_2:\text{Ce}^{3+}$, Eu^{2+} , Mn^{2+} phosphor. Such energy transfer occurs by way of a short-range interaction mechanism into $\text{Ce}^{3+}\text{--Eu}^{2+}$ and $\text{Ce}^{3+}\text{--Mn}^{2+}$ clusters formed in the crystalline matrix. In contrast to the $\text{Eu}^{2+} \rightarrow \text{Mn}^{2+}$ energy transfer usually observed in $\text{CaF}_2:\text{Eu}^{2+}:\text{Mn}^{2+}$, manganese ions do not appear to be sensitized by europium ions, which might suggest that Eu^{2+} ions prefer to cluster with tetragonal Ce^{3+} ions when these ions are also present in the lattice [22]. Table 2.4 summarizes four examples of the representative single-phased white-emitting phosphors with multiple energy transfer.

Regarding the mechanism, we shall describe two types of triply-doped white-emitting phosphor systems to illustrate the generation of white light through energy-transfer couples. First, the energy-level scheme illustrating the energy-transfer models of $\text{Ce}^{3+} \rightarrow \text{Tb}^{3+}$ and $\text{Ce}^{3+} \rightarrow \text{Mn}^{2+}$ in the $\text{Ce}^{3+}/\text{Mn}^{2+}/\text{Tb}^{3+}$ system is summarized in Fig. 2.9 [27].

Table 2.4 Single-phased white-emitting phosphors with multiple energy transfer

Phosphor	$\text{Ca}_3\text{Y}(\text{GaO})_3(\text{BO}_3)_4$: Ce^{3+} , Tb^{3+} , Mn^{2+}	$\text{Mg}_2\text{Y}_8(\text{SiO}_4)_6\text{O}_2$: Ce^{3+} , Tb^{3+} , Mn^{2+}	NaCaBO_3 : Ce^{3+} , Tb^{3+} , Mn^{2+}	$\text{BaMg}_2\text{Al}_6\text{Si}_9\text{O}_{30}$: Eu^{2+} , Tb^{3+} , Mn^{2+}
Excitation wavelength (nm)	365 (UV)	324 (UV)	347 (UV)	330 (UV)
Emission Wavelength (nm)	409 (V-B), 544 (G), 589 (O)	456 (B), 544 (G), 613 (R)	427 (B), 545 (G), 600 (R)	450 (B), 542 (G), 610 (R)
Energy transfer mechanism	Dipole–quadrupole (Ce^{3+} – Mn^{2+}) Dipole–quadrupole (Ce^{3+} – Tb^{3+})	Dipole–quadrupole (Ce^{3+} – Mn^{2+}) Dipole–quadrupole (Ce^{3+} – Tb^{3+})	Dipole–quadrupole (Ce^{3+} – Mn^{2+}) Dipole–quadrupole (Ce^{3+} – Tb^{3+})	Dipole–quadrupole (Eu^{2+} – Mn^{2+}) Dipole–quadrupole (Eu^{2+} – Tb^{3+})
Energy transfer critical distance (Å)	10.3 (Ce^{3+} – Mn^{2+})	10.5 (Ce^{3+} – Mn^{2+})	NA	NA
Reference	[26]	[49]	[27]	[28]

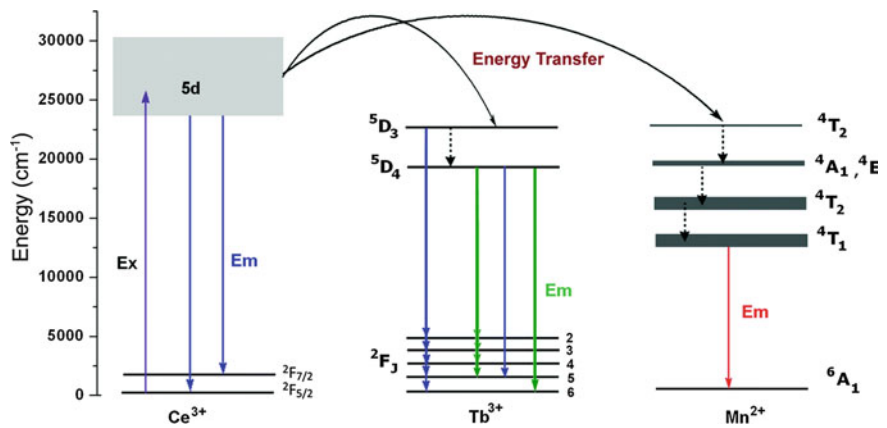


Fig. 2.9 Energy-level scheme illustrating the energy-transfer models of $\text{Ce}^{3+} \rightarrow \text{Tb}^{3+}$ and $\text{Ce}^{3+} \rightarrow \text{Mn}^{2+}$. Reproduced from Ref. [27] by permission of The Royal Society of Chemistry

In the ET model for $\text{Ce}^{3+}/\text{Tb}^{3+}/\text{Mn}^{2+}$ in various hosts, Ce^{3+} ions can be pumped from the $^2\text{F}_{5/2}$ ground state to the excited states by UV radiation and then transfer the energy to the Tb^{3+} $^5\text{D}_3$ level; subsequently, the $^5\text{D}_3$ level gives its characteristic transitions or continues to transfer the energy to the $^5\text{D}_4$ level by way of cross-relaxation. Then the green emission occurs from a set of characteristic optical transitions $^5\text{D}_4 \rightarrow ^7\text{F}_j$. The situation of the $\text{Ce}^{3+} \rightarrow \text{Mn}^{2+}$ energy transfer, which

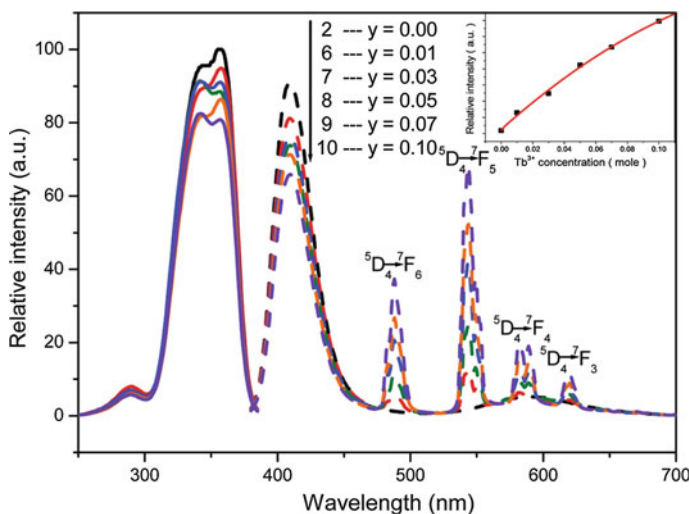


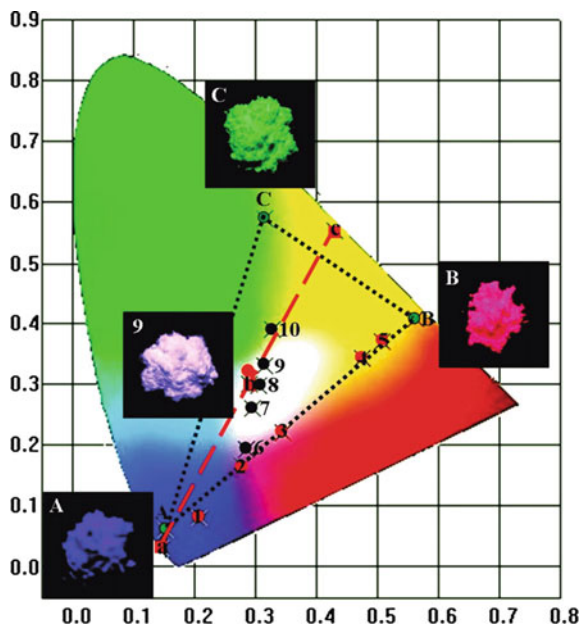
Fig. 2.10 Dependence of PL and PLE spectra of CYGB:0.01Ce³⁺, 0.03Mn²⁺, yTb³⁺ on y; the inset shows the relative PL intensity as a function of y at $\lambda_{\text{ex}} = 365$ nm. Reprinted with the permission from Ref. [26]. Copyright 2011 American Chemical Society

generates red emission, is similar: Mn²⁺ receives the energy transferred from excited Ce³⁺. The Mn²⁺ ion can be pumped from the ground state into its higher-energy levels. The excited state then relaxes to the excited state of ⁴T₁ (⁴G) through ⁴E (⁴D), ⁴T² (⁴D), (⁴E, ⁴A₁) (⁴G) and ⁴T₂ (⁴G) intermediate energy levels in a nonradiative process followed by a radiative transition from the excited state of ⁴T₁ (⁴G) to the ground state of ⁶A₁ (⁶S), thus giving rise to the typical emission of Mn²⁺ attributed to ⁴T₁ → ⁶A₁ in the host lattice. Three examples of white light-emitting phosphors are illustrated below.

- (a) Single-phased white-emitting Ca₃Y(GaO)₃(BO₃)₄:Ce³⁺, Mn²⁺, Tb³⁺ phosphor. The first novel single-composition white-emitting phosphor is a galloborate. Ca₃Y(GaO)₃(BO₃)₄:Ce³⁺, Mn²⁺, Tb³⁺, which has been reported by Huang et al. [26]. Figure 2.10 reports the dependence of PL and PLE spectra of Ca₃Y(GaO)₃(BO₃)₄:0.01Ce³⁺, 0.03Mn²⁺, yTb³⁺ on y, and the inset shows the relative PL intensity as a function of y at $\lambda_{\text{ex}} = 365$ nm. The spectral overlap between the Ce³⁺ emission band and the Mn²⁺ excitation band supports the occurrence of energy transfer from Ce³⁺ to Mn²⁺. This phosphor has been investigated and found to be a resonant type by way of a dipole–quadrupole mechanism. Because there is no spectral overlap between the PL spectrum of Ce³⁺ and PLE spectrum of Tb³⁺ in Huang’s work, no energy transfer from Ce³⁺ to Tb³⁺ was observed, thus indicating that Ce³⁺ and Tb³⁺ were co-excited simultaneously.

Through effective resonance-type energy transfer and co-excitation, the chromaticity coordinates of Ca₃Y(GaO)₃(BO₃)₄:Ce³⁺, Mn²⁺, Tb³⁺ phosphors

Fig. 2.11 Representation of the CIE chromaticity coordinates of CYGB:0.01Ce³⁺, xMn²⁺ (points 1 through 5), CYGB:0.01Ce³⁺ and CYGB:0.03Mn²⁺, yTb³⁺ (points 6 through 10). Reprinted with the permission from Ref. [26]. Copyright 2011 American Chemical Society



can be effectively tuned from (0.152, 0.061) for $\text{Ca}_3\text{Y}(\text{GaO})_3(\text{BO}_3)_4:\text{Ce}^{3+}$ to (0.562, 0.408) for $\text{Ca}_3\text{Y}(\text{GaO})_3(\text{BO}_3)_4:\text{Mn}^{2+}$, eventually reaching (0.314, 0.573) for $\text{Ca}_3\text{Y}(\text{GaO})_3(\text{BO}_3)_4:\text{Tb}^{3+}$. A WLED can be fabricated by using the white-emitting single-composition $(\text{Ca}_{0.97}\text{Mn}_{0.03})_3(\text{Y}_{0.92}\text{Ce}_{0.01}\text{Tb}_{0.07})(\text{GaO})_3(\text{BO}_3)_4$ pumped by a 365-nm U-chip. These results revealed that the CIE chromaticity coordinates and correlated color temperature (CCT) for white UV-LEDs were (0.31, 0.33) and 6524 K, respectively. Therefore, the white-emitting $\text{Ca}_3\text{Y}(\text{GaO})_3(\text{BO}_3)_4:\text{Ce}^{3+}$, Mn^{2+} , Tb^{3+} may serve as a promising material for phosphor-converted white-light UV-LEDs (Fig. 2.11).

- (b) White-emitting triply-doped $\text{Mg}_2\text{Y}_8(\text{SiO}_4)_6\text{O}_2:\text{Ce}^{3+}$, Mn^{2+} , Tb^{3+} phosphor [49]. The second triply-doped example deals with oxyapatite-type oxosilicate, $\text{Mg}_2\text{Y}_8(\text{SiO}_4)_6\text{O}_2$ (MYSO): Ce^{3+} , Mn^{2+} , Tb^{3+} , which was reported by Li et al. [49] In this research, the dual-energy transfer-induced $\text{Ce}^{3+}/\text{Mn}^{2+}/\text{Tb}^{3+}$ -triactivated MYSO phosphors were investigated. The investigators demonstrated that $\text{Ce}^{3+} \rightarrow \text{Mn}^{2+}$ energy transfer in MYSO: Ce^{3+} , Mn^{2+} phosphors is resonant type by way of a dipole-quadrupole mechanism, and the critical distances were found to be 10.5 and 9.7 Å, respectively, based on the calculation using both quenching-concentration and spectral-overlap methods. By the dual-energy transfer of $\text{Ce}^{3+} \rightarrow \text{Mn}^{2+}$ and $\text{Ce}^{3+} \rightarrow \text{Tb}^{3+}$, the emission colors of the investigated phosphors can be adjusted from blue to orange-red and from blue to green, respectively. Moreover, a wide-range tunable white light emission from cool to warm white with high quantum yields were obtained in $\text{Mg}_2\text{Y}_8(\text{SiO}_4)_6\text{O}_2:\text{Ce}^{3+}$, Mn^{2+} , Tb^{3+} samples by controlling the dopant

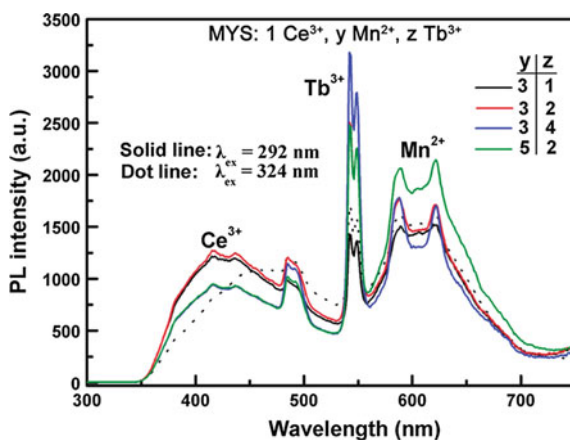


Fig. 2.12 PL spectra of MYSO: 1Ce^{3+} , $y\text{Mn}^{2+}$, $z\text{Tb}^{3+}$ samples ($y = 3, 5$ mol%; $z = 1, 2, 4$ mol%) under UV excitation: **a** 292 nm and **b** 324 nm. Reprinted with permission from Ref. [49]. Copyright 2011 American Chemical Society

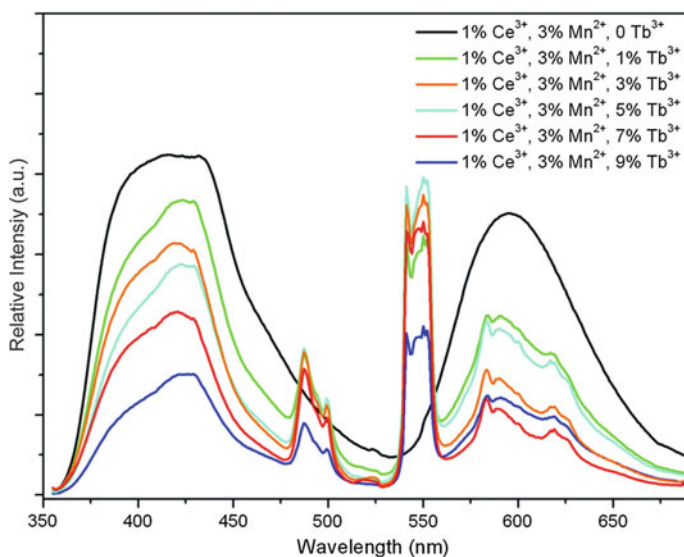


Fig. 2.13 Dependence of PL on Tb^{3+} content in $\text{NaCaBO}_3:1\%\text{Ce}^{3+}$, $3\%\text{Mn}^{2+}$, $z\%\text{Tb}^{3+}$ ($z = 0, 1, 3, 5, 7, 9$). Reproduced from Ref. [27] by permission of The Royal Society of Chemistry

contents of Ce^{3+} , Mn^{2+} , and Tb^{3+} ions. In addition, a color-tunable emission from $\text{MYSO}:\text{Ce}^{3+}$, Mn^{2+} , Tb^{3+} phosphors can be obtained by the modulation of excitation wavelength from 292 to 324 nm [49] (Fig. 2.12).

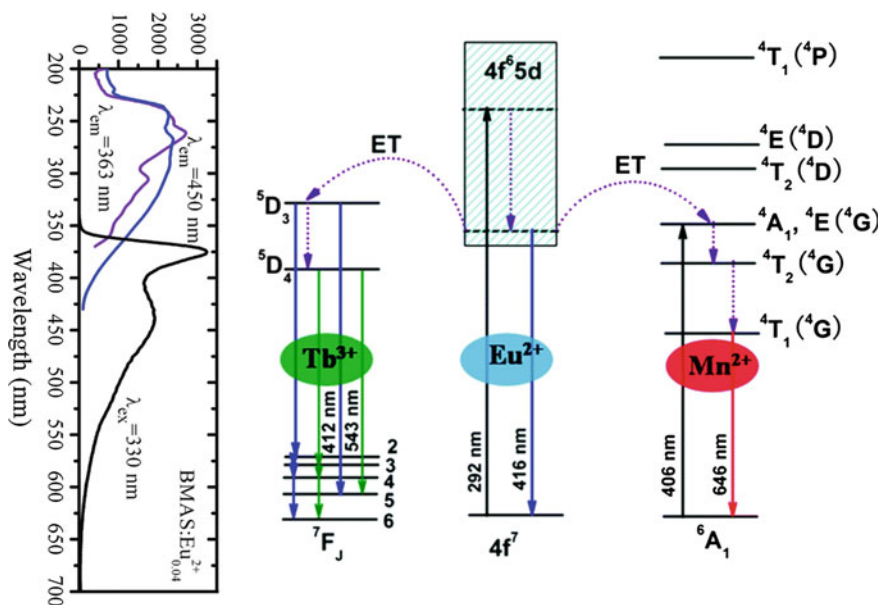


Fig. 2.14 Schematic-level diagram for the energy-transfer process in the BMASO:Eu²⁺, Tb³⁺, Mn²⁺ phosphor. The PLE ($\lambda_{\text{em}} = 450$ nm) and PL ($\lambda_{\text{ex}} = 330$ nm) spectra of BMASO:0.3%Eu²⁺ phosphor are also shown as a reference. Reprinted with permission from Ref. [50] by permission of The Royal Society of Chemistry

The investigators also demonstrated that a wide-range tunable white light emission from cool to warm white with high quantum yields (37–47 %) could also be obtained by properly controlling the contents of the three dopants [49].

- (c) White-emitting triply-doped NaCaBO₃:Ce³⁺, Mn²⁺, Tb³⁺ phosphor. The single-phased tri-chromatic white light-emitting phosphor NaCaBO₃:Ce³⁺, Mn²⁺, Tb³⁺ was reported by Zhang and Gong [27]. A wide-range-tunable trichromatic emission was obtained by precisely controlling the Ce³⁺, Mn²⁺, and Tb³⁺ dopant contents, which is attributed to the efficient resonance-type Ce³⁺→Tb³⁺/Ce³⁺→Mn²⁺ energy-transfer processes. Figure 2.13 shows the dependence of PL on Tb³⁺ content in NaCaBO₃:1%Ce³⁺, 3%Mn²⁺, *z*%Tb³⁺ (*z* = 0, 1, 3, 5, 7, 9) and the optimization of dopant compositions. The optimal composition of the phosphor was found to be NaCaBO₃:1%Ce³⁺, 3%Mn²⁺, 5%Tb³⁺, which emits white light on a 347-nm near-UV excitation. This white emission has a lower color temperature of 4898 K, and its CIE coordinates (0.344, 0.313) are closer to those of warm white light.
- (d) White-emitting triply-doped BaMg₂Al₆Si₉O₃₀:Eu²⁺, Tb³⁺, Mn²⁺ phosphor [28]. The second type of triply-doped white-emitting phosphor contains mainly a Eu²⁺/Tb³⁺/Mn²⁺ or Eu²⁺→Tb³⁺/Eu²⁺→Mn²⁺ system to generate white light through the energy-transfer process. Figure 2.14 illustrates the relative energy level schemes of Eu²⁺/Tb³⁺/Mn²⁺ and the possible

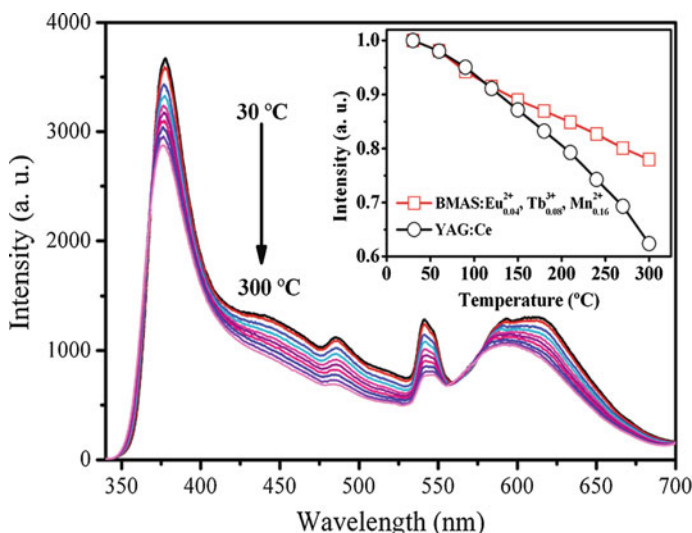


Fig. 2.15 Temperature-dependent emission spectra of the optimized BMAS:4% Eu^{2+} , 8% Tb^{3+} , 16% Mn^{2+} sample. Reprinted with the permission from Ref. [28]. Copyright 2011 American Chemical Society

energy-transfer models for $\text{Eu}^{2+} \rightarrow \text{Tb}^{3+}$ and $\text{Eu}^{2+} \rightarrow \text{Mn}^{2+}$ in a variety of hosts [50]. The PLE ($\lambda_{\text{em}} = 450 \text{ nm}$) and PL ($\lambda_{\text{ex}} = 330 \text{ nm}$) spectra of $\text{BaMg}_2\text{Al}_6\text{Si}_9\text{O}_{30}:\text{Eu}^{2+}, \text{Tb}^{3+}, \text{Mn}^{2+}$ is also shown on the left in Fig. 2.14 as a reference.

As shown in Fig. 2.14, the $5d$ band of Eu^{2+} overlaps partially the excited-state energy levels of Mn^{2+} ($^4\text{A}_1$, ^4E (^4G)) and Tb^{3+} ($^5\text{D}_3$), thus indicating that the two energy-transfer processes, $\text{Eu}^{2+} \rightarrow \text{Mn}^{2+}$ and $\text{Eu}^{2+} \rightarrow \text{Tb}^{3+}$, may occur by way of a nonradiative transition. When the Eu^{2+} ion is excited to higher component of $5d$ level by UV light, it relaxes to the lowest $5d$ crystal field-splitting level non-radiatively, and consequently it returns to the ground state ($4f^7$) with a 450-nm emission. Because they have similar values of energy levels, an energy transfer is expected to take place from the excited $5d$ state of Eu^{2+} to $^4\text{A}_1$, ^4E (^4G) level of Mn^{2+} and $^5\text{D}_3$ level of Tb^{3+} in the $\text{BaMg}_2\text{Al}_6\text{Si}_9\text{O}_{30}$ host. The Mn^{2+} ion receives the energy transferred from the excited Eu^{2+} , and the Mn^{2+} ion is then excited into the $^4\text{A}_1$ and ^4E (^4G) energy levels from the ground state. Furthermore, the excited Mn^{2+} relaxes to the excited $^4\text{T}_1$ (^4G) state through $^4\text{T}_2$ (^4G) intermediate energy level in a nonradiative process followed by a radiative transition from excited state of $^4\text{T}_1$ (^4G) to the ground state of $^6\text{A}_1$ (^6S) with a typical emission of Mn^{2+} located at 610 nm [28]. The $\text{Eu}^{2+} \rightarrow \text{Tb}^{3+}$ energy transfer is similar to the $\text{Eu}^{2+} \rightarrow \text{Mn}^{2+}$ energy transfer. The excited Eu^{2+} ions transfer energy to the $^5\text{D}_3$ level of Tb^{3+} ions; subsequently, the $^5\text{D}_3$ level gives its characteristic transitions or continues to transfer the energy to the $^5\text{D}_4$ level by way of cross-relaxation. Then a set of characteristic transitions of $^5\text{D}_4 \rightarrow ^7\text{F}_{3-6}$ attributed to Tb^{3+} are observed. By properly

tuning the relative composition of $\text{Tb}^{3+}/\text{Mn}^{2+}$ in $\text{BaMg}_2\text{Al}_6\text{Si}_9\text{O}_{30}:\text{Eu}^{2+}$, Tb^{3+} , Mn^{2+} , the chromaticity coordinates of (0.31, 0.30), high color-rendering index $R_a = 90$, and correlated color temperature (CCT) = 5,374 K can be achieved on the excitation of UV light. Figure 2.15 shows the temperature-dependent PL spectra of to investigate the thermal-quenching behavior of $\text{BaMg}_2\text{Al}_6\text{Si}_9\text{O}_{30}:4\%\text{Eu}^{2+}$, 8% Tb^{3+} , 16% Mn^{2+} . This investigation reveals excellent quenching characteristics of the current phosphors better than that of YAG:Ce.

2.5 Summary and Perspectives

In summary, this chapter has reviewed four categories of single-phased white light-emitting phosphors with potential applications for WLEDs. We have also proposed the design protocols on the basis of bonding nature of hosts and the resonant-type energy-transfer principle described previously. The luminescence properties and energy-transfer processes for the four types of singled-composition phosphors and a multi-composition phosphor have been discussed. As a result, light emission can be realized by adopting single-composition two-complementary or three-primary phosphors under ultraviolet excitation such as blue/yellow-emitting ($\text{CaAl}_2\text{Si}_2\text{O}_8:\text{Eu}^{2+}$, Mn^{2+}), aqua/red-emitting ($\text{BaGa}_4\text{S}_7:\text{Eu}^{2+}$, Mn^{2+}), or blue/green/red-emitting ($\text{SrZn}_2(\text{PO}_4)_2:\text{Eu}^{2+}$, Mn^{2+}) phosphors. On the other hand, white-light generation can also be realized by blue radiation coupled with a green-yellow/red-emitting phosphor ($\text{Ba}_2\text{ZnS}_3:\text{Ce}^{3+}$, Eu^{2+}), which will generate warm white light under ultraviolet excitation. Based on the observed significant overlap between the emission spectrum of the sensitizer and the excitation spectrum of the activator, the energy-transfer mechanism is undoubtedly an electric dipole–dipole interaction when the sensitizer and activator are both allowed transitions, e.g., the $\text{Ce}^{3+}/\text{Eu}^{2+}$ couple, whereas the electric dipole–quadrupole or exchange interaction occurs when the sensitizer and activator are allowed and forbidden transitions, respectively, e.g., the $\text{Eu}^{2+}/\text{Mn}^{2+}$ couple. In general, the magnitude of critical distance for energy transfer can be compared and listed as electric dipole–dipole > electric dipole–quadrupole > exchange interaction. The most intriguing examples of white-light generation with high color-rendering index (R_a) through resonant energy transfer are trichromatic inorganic phosphors to convert ultraviolet (UV), near-UV, or blue light into a combination of RGB.

In the investigation of energy transfer in inorganic phosphors, the mismatch in decay lifetimes among the sensitizers and the activators has been noticed, and the effect of decay mismatching on the efficiency of energy transfer from the sensitizer to the activator is beyond the scope of this discussion and requires detailed studies in the future.

Acknowledgments We acknowledge the generous financial support to this research from the Ministry of Science and Technology of Taiwan (ROC) during the past years. Part of the content

here is adapted from the Ph.D. dissertation of Dr. Yoan-Jen Yang of Department of Applied Chemistry, National Chiao Tung University, Taiwan.

References

1. Shimizu Y, Sakano K, Noguchi Y, Moriguchi T (1998) Japan Patent 10-56208
2. Bogner G, Botty IG, Braune B, Hintzen HT, van Krevel JWH, Waitl G (2003) Light source using a yellow-to-red-emitting phosphor. United States Patent 6,649,946
3. Hideki M, Koji K, Akihiko S (1999) Japan Patent 19990132924
4. Ropp RC (2004) Luminescence and the solid state, 2nd edn. Elsevier Publishers B. V., The Netherlands
5. Blasse G, Grabmaier BC (1994) Luminescent materials. Springer, Berlin, p 91
6. Douglas BE, McDaniel DH, Alexander JJ (1994) Concepts and models of inorganic chemistry, 3rd edn. Wiley, New York
7. Bartolo BD (1968) Optical interactions in solids. Wiley, New York
8. Dexter DL (1953) A theory of sensitized luminescence in solids. J Chem Phys 21:836
9. Blass G (1969) Energy transfer in oxidative phosphors. Philips Res Repts 24:131
10. Barry TL (1970) Luminescent properties of Eu^{2+} and $\text{Eu}^{2+} + \text{Mn}^{2+}$ activated $\text{BaMg}_2\text{Si}_2\text{O}_7$. J Electrochem Soc 117:381
11. Rubio JO, Murrieta HS, Powell RC, Sibley WA (1985) $\text{Eu}^{2+} \rightarrow \text{Mn}^{2+}$ energy transfer in NaCl. Phys Rev B 31:59
12. Rubio JO, Munoz FA (1987) Energy transfer between europium and manganese close pairs in monocrystalline sodium bromide. Phys Rev B 36:8115
13. Rubio JO (1989) $\text{Eu}^{2+} \rightarrow \text{Mn}^{2+}$ energy transfer in monocrystalline NaCl and NaBr. Phys Rev B 39:1962
14. Camarillo E, Rubio JO (1989) A spectroscopic study of NaI containing europium and manganese. J Phys: Condens Matter 1:4873
15. Caldino UG, Munoz AF, Rubio JO (1990) Luminescence and energy transfer in CaF_2 slightly doped with europium and manganese. J Phys: Condens Matter 2:6071
16. Caldino UG, Munoz AF, Rubio JO (1993) Energy transfer in CaCl_2 : Eu: Mn crystals. J Phys: Condens Matter 5:2195
17. Mendez A, Ramos FL, Riveros H, Camarillo E, Caldino UG (1999) Energy transfer mechanisms in the KBr: Eu^{2+} : Mn^{2+} phosphor. J Mater Sci Lett 18:399
18. Lin H, Liu X (1996) Chinese. J Lumin 17:121
19. Tan Y, Shi C (1999) $\text{Ce}^{3+} \rightarrow \text{Eu}^{2+}$ energy transfer in BaLiF_3 phosphor. J Phys Chem Solids 60:1805
20. Najafov H, Kato A, Toyota H, Iwai K, Bayramov A, Iida S (2002) Effect of Ce co-doping on CaGa_2S_4 : Eu phosphor: I. energy transfer from Ce to Eu ions. Jpn J Appl Phys 41:1424
21. Lin H, Liu XR, Pun EYB (2002) Sensitized luminescence and energy transfer in Ce^{3+} and Eu^{2+} codoped calcium magnesium chlorosilicate. Opt Mater 18:397
22. Caldino UG (2003) Energy transfer in CaF_2 doped with Ce^{3+} , Eu^{2+} and Mn^{2+} ions. J Phys: Condens Matter 15:7127
23. Setlur AA, Srivastava AM, Comanzo HA, Doxsee DD (2004) Phosphor blends for generating white light from near-UV/blue light-emitting devices. The United States Patent 6,685,852
24. Kim JS, Jeon PE, Choi JC, Park HL, Mho SI, Kim GC (2004) Warm-white-light emitting diode utilizing a single-phase full-color $\text{Ba}_3\text{MgSi}_2\text{O}_8$: Eu^{2+} , Mn^{2+} phosphor. Appl Phys Lett 84:2931
25. Kim JS, Jeon PE, Park YH, Choi JC, Kim HL, Kim GC, Kim TW (2004) White-light generation through ultraviolet-emitting diode and white emitting phosphor. Appl Phys Lett 85:3696

26. Huang CH, Chen TM (2011) A novel single-Composition trichromatic white-light $\text{Ca}_3\text{Y}(\text{GaO})_3(\text{BO}_3)_4$: Ce^{3+} , Mn^{2+} , Tb^{3+} phosphor for UV-LED. *J Phys Chem C* 115(5):2349
27. Zhang X, Gong M (2014) Single-phased white-light-emitting NaCaBO_3 : Ce^{3+} , Tb^{3+} , Mn^{2+} phosphors for LED applications. *Dalton Trans* 43:2465
28. Lü W, Zhang Z, Zhang X, Luo Y, Wang C, Zhang J (2011) Tunable full-color emitting $\text{BaMg}_2\text{Al}_6\text{Si}_9\text{O}_{30}$: Eu^{2+} , Tb^{3+} , Mn^{2+} phosphors based on energy transfer. *Inorg Chem* 50:7846
29. Shannon RD, Prewitt CT (1969) Effective ionic radii in oxides and fluorides. *Acta Crystallogr B* 25:925
30. Yao GQ, Lin JH, Zhang L, Lu GX, Gong ML, Su MZ (1998) Luminescent properties of $\text{BaMg}_2\text{Si}_2\text{O}_7$: Eu^{2+} , Mn^{2+} . *J Mater Chem* 8:585
31. Yang WJ, Chen TM (2005) Luminescence of Eu- and Mn-coactivated $\text{CaAl}_2\text{Si}_2\text{O}_8$ as a potential white-light phosphor for UVLED. *Chem Mater* 17:3883
32. Yang WJ, Chen TM (2006) Luminescence and energy transfer of Eu- and Mn-coactivated $\text{SrZn}_2(\text{PO}_4)_2$ as a single-composition white-emitting phosphor for UVLEDs. *Appl Phys Lett* 88(10):101903
33. Yang WJ, Chen TM (2006) Unpublished results
34. Chang CK, Chen TM (2007) White-light generation under violet-blue excitation from tunable green-to-red emitting $\text{Ca}_2\text{MgSi}_2\text{O}_7$: Eu, Mn through energy transfer. *Appl Phys Lett* 90(16):161901
35. Chang K, Chen TM (2007) Unpublished results
36. Liu WR, Chiu YC, Yeh YT, Jang SM, Chen TM (2009) Luminescence and energy transfer mechanism in $\text{Ca}_{10}\text{K}(\text{PO}_4)_7$: Eu^{2+} , Mn^{2+} phosphor. *J Electrochem Soc* 156(7):J165
37. Huang CH, Chen TM (2010) $\text{Ca}_9\text{La}(\text{PO}_4)_7$: Eu^{2+} , Mn^{2+} : an emission-tunable phosphor through efficient energy transfer for white light-emitting diodes. *Opt Express* 18(5):5089
38. Huang CH, Chen TM, Liu WR, Chiu YC, Yeh YT, Jang SM (2010) A single-phased emission-tunable phosphor $\text{Ca}_9\text{Y}(\text{PO}_4)_7$: Eu^{2+} , Mn^{2+} with efficient energy transfer for white light-emitting diodes. *ACS Appl Mater Interf* 2(1):259
39. Huang CH, Liu WR, Chen TM (2010) Single-phased white-light phosphors $\text{Ca}_9\text{Gd}(\text{PO}_4)_7$: Eu^{2+} , Mn^{2+} under near-ultraviolet excitation. *J Phys Chem C* 114:18698
40. Huang CH, Chan TS, Liu WR, Wang DY, Chiu YC, Yeh YT, Chen TM (2012) Crystal structure and blue-white-yellow color-tunable $\text{Ca}_4\text{Si}_2\text{O}_7\text{F}_2$: Eu^{2+} , Mn^{2+} phosphor through energy transfer for single-phased white-light near-ultraviolet LEDs. *J Mater Chem* 22:20210
41. Yang WJ, Chen TM (2007) $\text{Ce}^{3+}/\text{Eu}^{2+}$ codoped Ba_2ZnS_3 : a blue radiation-converting phosphor for white light-emitting diodes. *Appl Phys Lett* 90(17):171908
42. Chang CK, Chen TM (2007) Unpublished results
43. Xiao F, Xue YN, Zhang QY (2009) $\text{Ca}_2\text{BO}_3\text{Cl}$: Ce^{3+} , Eu^{2+} : a potential tunable yellow-white-blue-emitting phosphors for white light-emitting diodes. *Phys B* 404:3743
44. Chang CK, Chen TM (2007) $\text{Sr}_3\text{B}_2\text{O}_6$: Ce^{3+} , Eu^{2+} : a potential single-phased white-emitting borate phosphor for ultraviolet light-emitting diodes. *Appl Phys Lett* 91(8):081902
45. Hsu CH, Das S, Lu CH (2012) Color-tunable, single-phased $\text{MgY}_4\text{Si}_3\text{O}_{13}$: Ce^{3+} , Mn^{2+} phosphors with efficient energy transfer for white-light-emitting diodes. *J Electrochem Soc* 159(5):J193
46. Müller M, Jüstel T (2014) On the luminescence and energy transfer of white emitting $\text{Ca}_3\text{Y}_2(\text{Si}_3\text{O}_9)_2$: Ce^{3+} , Mn^{2+} phosphor. *J Lumin* 155:398
47. Liu Y, Xia Zhang X, Hao Z, Wang X, Zhang J (2011) Tunable full-color-emitting $\text{Ca}_3\text{Sc}_2\text{Si}_3\text{O}_{12}$: Ce^{3+} , Mn^{2+} phosphor via charge compensation and energy transfer. *Chem Commun* 47:10677
48. Li G, Geng D, Sheng M, Peng C, Cheng Z, Lin J (2011) Tunable luminescence of $\text{Ce}^{3+}/\text{Mn}^{2+}$ -coactivated $\text{Ca}_2\text{Gd}_8(\text{SiO}_4)_6\text{O}_2$ through energy transfer and modulation of excitation: potential single-phase white/yellow-emitting phosphors. *J Mater Chem* 21:13334

49. Li G, Geng D, Shang M, Zhang Y, Peng C, Cheng Z, Lin J (2011) Color tuning luminescence of $\text{Ce}^{3+}/\text{Mn}^{2+}/\text{Tb}^{3+}$ -triactivated $\text{Mg}_2\text{Y}_8(\text{SiO}_4)_6\text{O}_2$ via energy transfer: potential single-phase white-light-emitting phosphors. *J Phys Chem C* 115:21882
50. Jiang L, Pang R, Li D, Sun W, Jia Y, Li H, Fu J, Li C, Zhang S (2015) Tri-chromatic white-light emission from a single-phase $\text{Ca}_9\text{Sc}(\text{PO}_4)_7$: Eu^{2+} , Tb^{3+} , Mn^{2+} phosphor for LED applications. *Dalton Trans* 44:17241

Phosphors, Up Conversion Nano Particles, Quantum
Dots and Their Applications

Volume 1

Liu, R.-S. (Ed.)

2017, VIII, 593 p. 377 illus., 257 illus. in color.,

Hardcover

ISBN: 978-3-662-52769-6